Journal of Power Sources 193 (2009) 501–506

Contents lists available at ScienceDirect

Journal of Power Sources

journal homepage: www.elsevier.com/locate/jpowsour

Cyclic voltammetry and X-ray photoelectron spectroscopy studies of electrochemical stability of clean and Pt-modified tungsten and molybdenum carbide (WC and Mo_2C) electrocatalysts

Erich C. Weigert[a], Daniel V. Esposito[b], Jingguang G. Chen[b,*]

[a] Department of Materials Science and Engineering, Center for Catalytic Science and Technology (CCST), University of Delaware, Newark, DE 19716, United States
[b] Department of Chemical Engineering, Center for Catalytic Science and Technology (CCST), University of Delaware, 150 Academy St., Newark, DE 19716, United States

ARTICLE INFO

Article history:
Received 18 February 2009
Received in revised form 11 April 2009
Accepted 15 April 2009
Available online 23 April 2009

Keywords:
Carbides
WC
Mo_2C
Platinum
Electrocatalysts
Fuel cells

ABSTRACT

The electrochemical stability of tungsten carbide (WC), Pt-modified WC, molybdenum carbide (Mo_2C), and Pt-modified Mo_2C has been examined using an *in situ* electrochemical half-cell in combination with X-ray photoelectron spectroscopy (XPS). The WC surface, created via the carburization of a tungsten foil, was electrochemically stable to ~0.8 V with respect to the normal hydrogen electrode (NHE) when exposed to dilute sulfuric acid. At higher potentials, XPS confirmed the surface oxidation of WC to form W_xO_y species. The deposition of submonolayer coverage of Pt on the WC surface increased the region of stability of WC, extending the onset of catalyst oxidation to ~1.0 V (NHE). These results suggest that both WC and Pt/WC have the potential to be used as anode electrocatalysts. In contrast, both Mo_2C and Pt-modified Mo_2C underwent oxidation at ~0.4 V (NHE), indicating that molybdenum carbides are not stable enough for applications as anode electrocatalysts.

1. Introduction

This work is a continuation to a series of surface science and electrochemical studies attempting to evaluate the feasibility of using tungsten and molybdenum carbides as anode electrocatalysts for direct methanol fuel cell (DMFC) [1–7]. DMFC anodic chemistry requires the oxidation of methanol and the decomposition of water to produce protons, electrons, and gas-phase CO_2 [8]. In addition to meeting these requirements, a desirable DMFC electrocatalyst must remain stable under the relatively harsh environment at the anode. Currently, the Pt/Ru bimetallic catalyst is the most effective anode electrocatalyst for DMFC [9–11]. Although the Pt/Ru bimetallic system exhibits desirable stability and electrochemical activity under anodic conditions, both Pt and Ru are expensive due to limited supplies. In addition, strong chemisorption of CO on Pt and Ru makes the electrocatalyst susceptible to CO poisoning, blocking the active sites for methanol oxidation. Consequently, discovery of less expensive and more CO tolerant alternatives to the Pt/Ru catalysts would help facilitate the commercialization of DMFC.

A large body of literature exists on the possibility of using transition metal carbides to mimic the catalytic properties of Pt-group metals [12–18]. In particular, there have been many studies on tungsten and molybdenum carbides since Levy and Boudart suggested that WC displayed Pt-like behavior in several catalytic reactions [18]. There have also been many recent studies to utilize supported tungsten carbides as alternative electrocatalysts [5,6,19–29].

The earlier papers of this series examined the surface reactions of methanol, water, and CO on carbide-modified tungsten and molybdenum single crystal and polycrystalline surfaces, with and without submonolayer coverages of Pt [1–5,7]. The carbide surfaces showed high activity toward the dissociation of methanol and water, as well as a relatively low desorption temperature of CO at around 330 K, suggesting that tungsten and molybdenum carbides would be potential electrocatalysts to replace Pt/Ru for DMFC. Recent cyclic voltammetry (CV) and chronoamperometry (CA) measurements confirmed that tungsten monocarbide (WC) and Pt-modified WC were active for the electrooxidation of methanol [6].

One of the critical issues in using carbides as alternative electrocatalysts is their stability within an electrochemical environment. In particular, it is very important to understand whether the carbides are oxidized after electrochemical measurements. Although X-ray photoelectron spectroscopy (XPS) has been used to determine the oxidation state of tungsten or molybdenum after electrochem-

* Corresponding author. Tel.: +1 302 831 0642; fax: +1 302 831 2085.
E-mail addresses: weigeec@jmusa.com (E.C. Weigert), espo@udel.edu (D.V. Esposito), jgchen@udel.edu (J.G. Chen).

0378-7753/$ – see front matter © 2009 Elsevier B.V. All rights reserved.
doi:10.1016/j.jpowsour.2009.04.020

ical study, the samples in these previous studies were exposed to air between the electrochemical and XPS measurements, making it difficult to determine whether the oxidation occurred in air or during electrochemical evaluation. The focus of the current study is to clarify the uncertainties in the electrochemical stability of tungsten and molybdenum carbides using an *in situ* three-electrode half-cell that was connected via a gate valve to a UHV system containing XPS. This system allowed for surface characterization of carbides and Pt-modified carbides, both before and after CV measurements, without exposing the carbide electrode surfaces to air. Such measurements remove the potential complication due to air oxidation and therefore should provide conclusive evidence on the electrochemical stability of carbides.

2. Experimental

2.1. Techniques

The XPS measurements were performed in a UHV system equipped with an ESCALAB MK2 by VG Scientific Ltd, as described previously [6]. An Al Kα X-ray source of 1486.6 eV was used as the excitation source. All scans were performed with an anode potential of 12 kV and an emission current of 20 mA. The concentric hemispherical analyzer was mounted at 54.7° with respect to the X-ray source and XPS scans were taken under a vacuum condition of approximately 1×10^{-8} Torr.

The CV measurements were performed using a three-electrode electrochemical half-cell, consisting of a counter (auxiliary) electrode, a reference electrode, and a working electrode. As shown in Fig. 1, the half-cell assembly was attached to the UHV chamber via a gate valve. Implementation of the load lock transfer system between the electrochemical half-cell and the UHV chamber eliminated exposure of the sample to air during and after CV measurements. The counter electrode of the electrochemical half-cell was 99.99% pure Pt gauze, 0.1 mm thick with a surface area of approximately 15 cm^2. The reference electrode was a saturated calomel electrode ($Hg/Hg_2Cl_2/KCl$), which was measured to be 0.241 V with respect to the normal hydrogen electrode (NHE). The working electrode, typically a metal foil with a surface area of 1 cm^2, was the electrocatalyst (WC or Mo_2C with or without Pt modification) under investigation. The working electrode was spot welded onto a stainless steel feedthrough, allowing only the electrocatalyst to come in contact with the electrolyte of the electrochemical half-cell. The stainless steel feedthrough was connected to a Princeton Applied Research model 263A potientostat/galvanostat that controlled the potentials of the electrodes. The half-cell used 0.05 M H_2SO_4 as an electrolyte that was continuously pumped in a closed loop at ~10 ml min^{-1} from a 2.0-L glass vessel. A linear potential sweep between the working electrode and reference electrode, from −0.09 V to the desired potential then back to −0.09 V with respect to the NHE at 100 mV s^{-1}, was performed using the potentiostat.

To eliminate exposure of the sample to air during CV measurements and sample transfer to and from the XPS chamber, a typical experiment proceeded as follows, similar to that developed by Goodman and coworkers [30] and Stuve and coworker [31]. The metal carbide surface was first prepared and characterized using XPS in the UHV chamber. The sample was then positioned in the load lock chamber under vacuum and separated from the UHV chamber by closing a gate valve. The pressure inside the load lock chamber was raised to 1 atm using 99.999% purity N_2 and the gate valve was opened between the load lock chamber and electrochemical half-cell, which was pre-evacuated and backfilled with 99.999% purity N_2. The electrochemical half-cell was raised to allow the meniscus of the electrolyte to contact the surface of the sample. The electrolyte/fuel mixture was then pumped through the cell at 10 ml min^{-1} from a 2-L reservoir, which was purged with N_2. By raising the electrochemical half-cell, the tip of the Luggin-Haber capillary attached to the reference electrode was also brought near the surface, allowing CV measurements to be performed. Following CV measurements, the electrochemical half-cell was retracted, the gate valve to separate the load lock chamber from the electrochemical half-cell was closed, and the load lock chamber was evacuated to UHV conditions. Finally, the gate valve to the UHV chamber was opened and post-CV characterization was performed using XPS.

2.2. Preparations of clean and Pt-modified WC and Mo_2C thin films

To create the WC or Mo_2C thin films, a polycrystalline metal foil (either W or Mo) was carburized by decomposition of ethylene over a hot filament and deposition of the carbon on the metal surface, followed by annealing the sample to 1200 K. Prior to carburization, the surface of a 1 cm × 1 cm × 0.05 mm metal foil (99.9+% purity purchased from Aldrich Chemical Company Inc.) was cleaned by cycles of Ar^+ bombardment at 300 K (sample current ~5 μA, acceleration potential 4 kV) followed by flashing to 1200 K in vacuum. This 10-min cycle was generally repeated 2 times. XPS analysis after the cleaning cycles showed no detectable amount of impurities on the W or Mo surface. To carburize the clean W or Mo surface, 1.0×10^{-4} Torr of ethylene was decomposed using a hot filament sputter gun with 0.5 kV bias potential for 10 min. The surface was then annealed to 1200 K to form a carbide film. Several cycles of carburization were used to assure the formation of carbide films. XPS analysis revealed the characteristic carbidic carbon 1s feature at ~282.7 eV and an atomic C/W ratio of 1.0 (or C/Mo ~ 0.5) with no detectable impurities.

The Pt-modified surfaces were prepared via the evaporation of elemental Pt onto the clean carbide thin film [6]. The deposition of Pt was achieved by resistively heating a tungsten filament that was wrapped with a thin wire of 99.99+% pure Pt. The Pt evaporation source was contained within a tantalum shield, which had an aperture to direct Pt onto the carbide thin film surface without contaminating the entire UHV chamber. The metal thin film was maintained at 300 K during deposition followed by annealing to 600 K for 1 min after Pt deposition. The surface coverage of atomic Pt was estimated based on the Pt(4f)/W(4f) or Pt(4f)/Mo(3d) XPS ratio along with the standard XPS sensitivity factors as described elsewhere [32]. The calculations took into consideration screening of the W or Mo XPS signal by the surface Pt atoms and the contribution of the signal from metal layers in the bulk. After the Pt deposition rate was established based on the monolayer (ML) Pt layer on the clean metal foil, a similar deposition rate was used to form Pt-modified WC or Mo_2C surfaces with controlled amounts of Pt, ranging from 0.8 ML (monolayer) to 1.2 ML.

3. Results

3.1. Characterization of WC thin film

3.1.1. XPS and XRD results

Fig. 2 compares the W 4f and C 1s XPS spectra of a polycrystalline tungsten foil before and after the formation of the WC thin film. The WC film is characterized by tungsten $4f_{7/2}$ and $4f_{5/2}$ features at 31.6 and 33.7 eV, and a carbidic C 1s feature at 282.7 eV. There are no other impurities, such as oxygen or sulfur (spectra not shown), on the WC surface. The comparison of the W 4f region also shows that binding energies of the two W 4f features increase by about ~0.3 eV from clean W to WC, suggesting that the oxidation state of W is slightly higher upon the formation of WC.

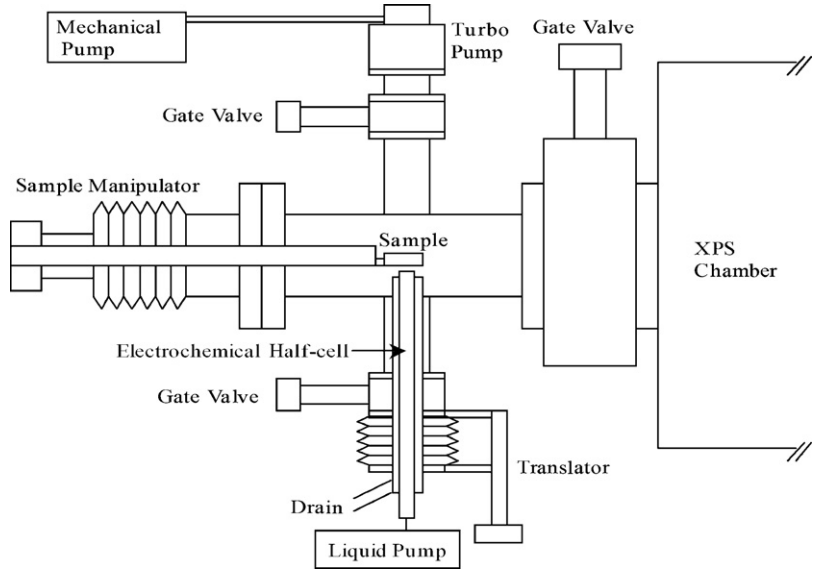

Fig. 1. Schematic of the combined electrochemical half-cell and XPS system.

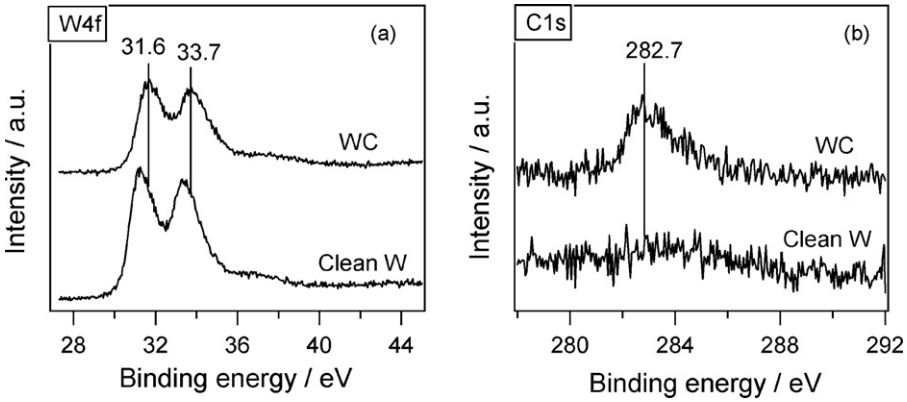

Fig. 2. (a) W 4f and (b) C 1s XPS spectra of a polycrystalline W foil before and after carburization in vacuum.

The tungsten to carbon atomic ratio, derived from the W 4f and C 1s peak areas and the corresponding sensitivity factors [26], is calculated to be 1.0, indicating that the surface stoichiometry is WC within the detection limit of XPS. The WC stoichiometry is confirmed in the GIXRD pattern of the carbide thin film in Fig. 3. Scanning 2θ from 10° to 70°, the WC film exhibits the following characteristic features: $2\theta = 31.5$, WC 0 0 1; $2\theta = 35.8$, WC 100; and $2\theta = 48.4$, WC 1 0 1. A very weak peak is observed at $2\theta = 39.4$, which is due to the presence of trace amounts of W_2C.

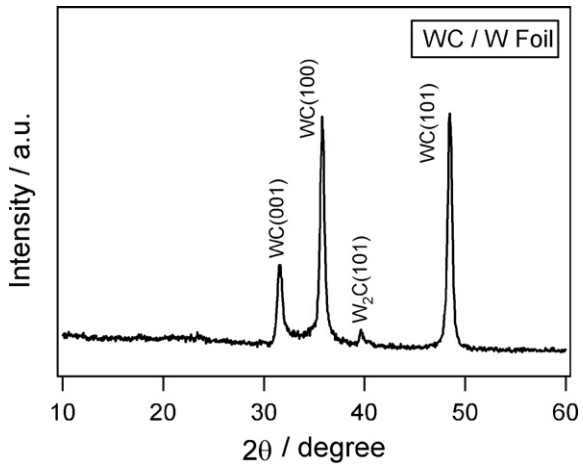

Fig. 3. GIXRD data of WC produced on a polycrystalline W foil.

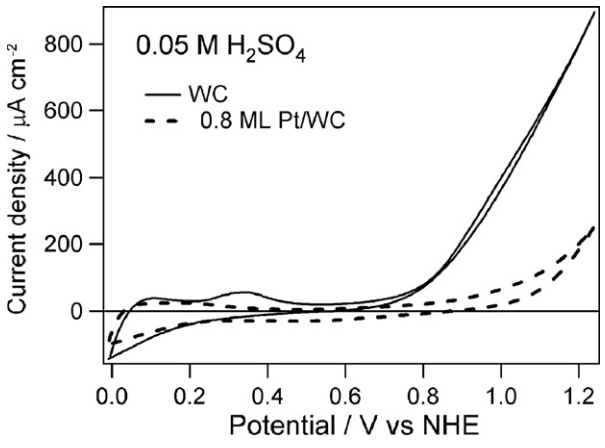

Fig. 4. Cyclic voltammetry curves of WC and 0.8 ML Pt/WC surfaces exposed to 0.05 M H_2SO_4.

3.1.2. Electrochemical stability of WC and Pt/WC surfaces in 0.05 M H_2SO_4

Fig. 4 displays CV curves for WC and ~0.8 ML Pt/WC thin film surfaces exposed to 0.05 M H_2SO_4. The samples were transferred directly from UHV to a nitrogen purged electrochemical half-cell via load/lock to eliminate exposure to air. For all CV measurements, the potentials are given with respect to the normal hydrogen electrode (NHE) and the anodic current was defined to be positive. The working electrode (WC or Pt/WC) was cycled from −0.09 to 1.241 V and back to −0.09 V at a linear rate of 100 mV s^{-1}. The CV curves in Fig. 4 were obtained after 30 cycles.

The CV curve of WC showed a cathodic current at −0.09 V due to the hydrogen evolution reaction (HER). Linearly increasing the potential, the WC surface displayed an anodic feature centered at ~0.27 V, most likely resulting from the oxidation of adsorbed H that was previously generated during the HER. Further increasing the potential from ~0.4 to ~0.8 V resulted in no significant electrochemical activity. Beyond 0.8 V, the onset of a significant oxidation current occurred and persisted to 1.241 V. This oxidation current is attributed to the irreversible oxidation of the WC film into W_xO_y species. As the potential of the WC working electrode was decreased, the curve retraced its path until the onset to a cathodic current at ~0.2 V, again due to the onset of the HER. In comparison, the CV curve of the 0.8 ML Pt/WC surface displayed enhanced catalyst stability in H_2SO_4. The onset voltage for oxidation increased from ~0.8 V for WC to ~1.0 V for 0.8 ML Pt/WC.

To confirm that the oxidation of WC into W_xO_y species occurred at potentials above 0.8 V, XPS was used in conjunction with CV to determine the surface oxidation states of W. Fig. 5a compares XPS spectra of the W 4f region after multiple CV cycles of the WC electrode in 0.05 M H_2SO_4 to 1.241 V. After 15 cycles, significant tungsten oxide features appeared at 35.8 and 37.9 eV. After an additional 15 cycles, growth of the oxide features continued, making oxides the dominant state of tungsten on the surface. Finally, after 70 cycles, only tungsten oxide features were detected using XPS.

Fig. 5b shows the XPS spectra of 0.8 ML Pt/WC and 1.2 ML Pt/WC surfaces after 50 CV cycles in 0.05 M H_2SO_4 to 1.241 V. Unlike the WC surface that showed significant tungsten oxide surface states after CV measurements to 1.241 V, the 0.8 ML Pt/WC and 1.2 ML Pt/WC surfaces displayed mostly carbidic tungsten $4f_{7/2}$ and $4f_{5/2}$ states at 31.6 and 33.7, respectively. The comparison in Fig. 5b also indicates that similar stabilization effect of WC is achieved at Pt coverages below a monolayer (0.8 ML) and above a monolayer (1.2 ML).

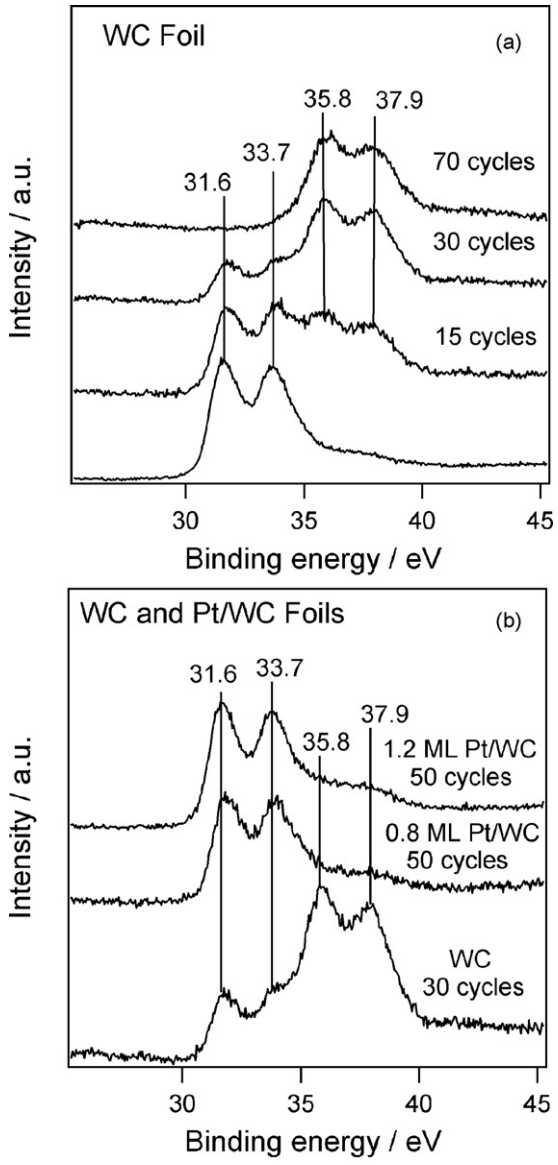

Fig. 5. XPS spectra of W 4f region from the (a) WC and (b) Pt/WC surfaces before and after CV measurements in 0.05 M H_2SO_4 to 1.241 V.

3.2. Characterization of Mo_2C thin film

3.2.1. XPS and XRD results

Fig. 6 compares the Mo 4d and C 1s XPS spectra of a polycrystalline molybdenum foil before and after the formation of the Mo_2C thin film. The Mo_2C film is characterized by Mo $3d_{5/2}$ and $3d_{3/2}$ features at 228.1 and 231.2 eV, and a carbidic C 1s feature at 282.9 eV. There are no other impurities, such as oxygen or sulfur (spectra not shown), on the Mo_2C film. Similar to that observed in Fig. 2 upon the formation of tungsten carbide, the comparison of the Mo 3d region also shows that binding energies of the two Mo features increase by about ~0.3 eV from clean Mo to Mo_2C, suggesting that the oxidation state of Mo is slightly higher upon the formation of Mo_2C.

The molybdenum to carbon atomic ratio, derived from the Mo 3d and C 1s peak areas and the corresponding sensitivity factors [33], is calculated to be 2.0, indicating that the surface stoichiometry is Mo_2C within the detection limit of XPS. The bulk Mo_2C stoichiometry is confirmed in the GIXRD pattern of the carbide thin film in Fig. 7, in which diffraction peaks appear corresponding to the hexagonal β-Mo_2C [34] phase. The XRD pattern also shows a single molybdenum reflection of the (2 0 0) plane from the deeper and un-carburized bulk portion of the molybdenum foil. The relatively weak intensity of the Mo diffraction peak also suggests that the Mo_2C film occupies a substantial portion of the sampling depth shown in this data.

3.2.2. Electrochemical stability of Mo_2C and Pt/Mo_2C surfaces in 0.05 M H_2SO_4

Fig. 8 displays CV curves for Mo_2C and ~0.8 ML Pt/Mo_2C thin film surfaces exposed to 0.05 M H_2SO_4. The working electrode (Mo_2C or Pt/Mo_2C) was cycled from −0.09 to 1.0 V and back to −0.09 V at a linear rate of 100 mV s^{-1}. The CV curves in Fig. 8 were obtained after 30 cycles.

The CV curve for Mo_2C suggests that the onset of anodic oxidation is located at a potential of ~0.4 V. Beyond this potential, the linear increase of the current response is indicative of an increasing rate of oxidation of the Mo_2C surface as the potential increases. What is distinct about the CV curves on Mo_2C is that the voltammograms do not decay after many CV cycles (not shown). In the case of irreversible oxidation of the electrocatalyst, the anticipated behavior [35] of the current response is that the linear region demonstrating the oxidation should decrease with each subsequent scan due to an increasing quantity of metal oxide produced on the

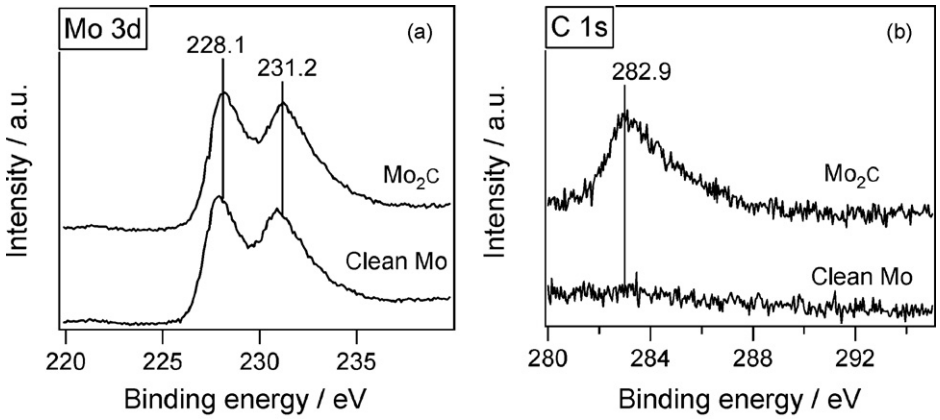

Fig. 6. (a) Mo 3d and (b) C 1s XPS spectra of a polycrystalline Mo foil before and after carburization in vacuum.

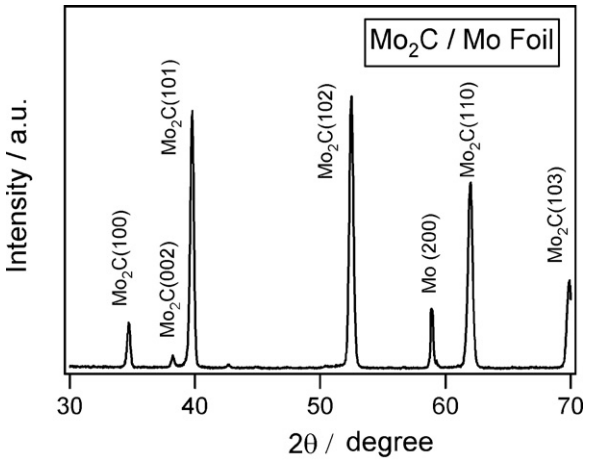

Fig. 7. GIXRD data of Mo_2C produced on a polycrystalline Mo foil.

surface. At the same time, broad anodic and cathodic peak features are expected to appear at lower potential regions, indicating a reversible change in metal oxidation state occurring on the surface with each potential sweep. The reproducibility of this current response for Mo_2C indicates that the oxidized Mo dissolves rapidly into solution after each potential cycle. The broad features that occur between 0 and ~0.3 V may be related to pseudo-capacitive effects [36] from MoO_x species formed during the potential cycling experiments.

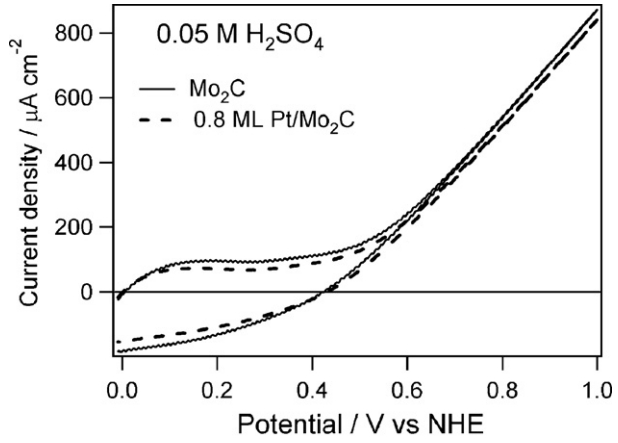

Fig. 8. Cyclic voltammetry curves of Mo_2C and Pt/Mo_2C surfaces exposed to 0.05 M H_2SO_4.

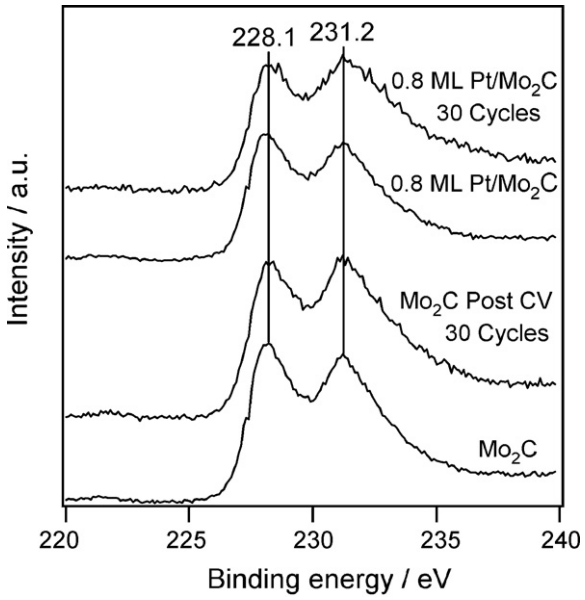

Fig. 9. Mo 3d XPS spectra of the Mo_2C and Pt/Mo_2C surfaces before and after CV studies in 0.05 M H_2SO_4 to 1.0 V.

The presence of potential synergistic contributions of Pt on the electrochemical response was studied by the metal evaporation of Pt on the Mo_2C foil surface, as shown in the dashed line in Fig. 8. The CV curves are approximately the same between Mo_2C and ~0.8 ML Pt/Mo_2C, with the onset of anodic oxidation being similar between the two surfaces. Unlike the observation of a Pt-enhanced stability for WC, the presence of submonolayer coverage of Pt does not increase the range of electrochemical stability of Mo_2C.

The Mo 3d XPS are compared for Mo_2C and ~0.8 ML Pt/Mo_2C before and after CV measurements in Fig. 9. One interesting observation is that the Mo peaks remain at 228.1 and 231.2 eV. Oxidized Mo features, which should appear at higher binding energies [26], are not observed. This is consistent with the CV results that indicate that the oxidized Mo species are dissolved into the solution during CV measurements. The comparison in Fig. 9 also indicates that the surface state of Mo_2C is similar with and without Pt, consistent with the similar CV curves in Fig. 8.

4. Discussion

The most desirable properties for a DMFC anode electrocatalyst include activity toward CH_3OH and/or CO oxidation and stability during fuel cell operation. Although tungsten and molybdenum

carbides both show activity toward CH_3OH oxidation, results from the current study clearly demonstrate the difference in stability between the two materials.

Previously, physical vapor deposition (PVD) has been used to create phase-pure WC and W_2C thin films on glassy carbon substrates via magnetron sputtering [5]. *Ex situ* CV and XPS measurements showed that the W_2C film was not stable in the electrochemical environment, oxidizing to form surface W_xO_y species at relatively low potentials [5]. In contrast, the PVD WC thin film showed promise as alternative anode electrocatalysts, demonstrating a region of stability under anodic conditions up to ~0.6–0.8 V with respect to the NHE [5]. This region of stability potentially allows for the oxidation of fuel, such as hydrogen or methanol, without the formation of surface W_xO_y species that could potentially block active electrocatalytic sites. The region of stability of the WC film is further confirmed in the current study from the *in situ* CV and XPS measurements in Figs. 4 and 5.

Furthermore, results from the current study also demonstrate the enhancement in the stability of WC surfaces upon the deposition of low coverages of Pt on WC. The CV curve of the 0.8 ML Pt/WC thin film exposed to 0.05 M H_2SO_4 (Fig. 4) clearly reveals an enhanced region of stability over the WC surface, showing an increase in the onset of oxidation to ~1.0 V (NHE). This conclusion is further supported by XPS spectra in Fig. 5b, which demonstrate the enhanced stability of the 0.8 ML Pt/WC and 1.2 ML Pt/WC surfaces after CV measurements to 1.241 V in 0.05 M H_2SO_4. Both Pt-modified WC surfaces show a significant decrease in the formation of tungsten oxide features as compared to that of the WC surface, indicating that the enhancement of the surface stability can be achieved at the submonolayer (0.8 ML) Pt coverage. The enhanced stability of the Pt/WC surface is attributed to the strong bonding between Pt and WC, most likely at defect regions of the WC surface, to prevent the surface oxidation. More detailed structural characterization, such as using scanning tunneling microscope (STM), is underway to determine the location and morphology of Pt on the WC surface.

In contrast, the CV and XPS results in Figs. 8 and 9 suggest facile oxidation of Mo_2C and subsequent dissolution of oxidized Mo into the electrolyte while the surface is exposed to anodic potentials above ~0.4 V. The deposition of submonolayer coverages of Pt does not enhance the electrochemical stability of Mo_2C. In addition to the obvious problems with the instability of Mo_2C, the dissolution of oxidized Mo could lead to the accumulation of Mo in the ionomer membrane and interfere with the performance of DMFC. Therefore, unlike WC, Mo_2C does not appear to possess the necessary stability to be used in DMFC.

5. Conclusions

From the results and discussion presented above, the following conclusions can be made regarding the stability of WC and Mo_2C films as electrocatalysts:

(1) The WC film shows a region of stability between 0 and ~0.8 V (NHE) when exposed to 0.05 M H_2SO_4. At potentials greater than ~0.8 V, WC oxidizes irreversibly into W_xO_y species as confirmed by the CV and XPS measurements.
(2) Modification by low coverages of Pt on the WC surface leads to an enhancement in the region of stability in H_2SO_4, increasing the oxidation potential of the electrocatalyst surface to ~1.0 V as confirmed by the CV and XPS measurements. Combining the current results with our previous CV and CA studies of the activity of Pt/WC for the oxidation of methanol, it is evident that Pt-modified WC can be a promising alternative electrocatalyst.
(3) In contrast, the region of stability for Mo_2C is significantly narrower, with irreversible oxidation and subsequent dissolution occurring at potentials greater than ~0.4 V (NHE). The deposition of Pt does not show an enhancement in the stability. These results indicate that Mo_2C might have very limited application as an electrocatalyst.

Acknowledgments

We acknowledge financial support from the National Science Foundation (Grant # CTS – 0518900). We also acknowledge partial support from the Department of Energy (Grant # DE-AC05-76RL01830).

References

[1] H.H. Hwu, J.G. Chen, K. Kourtakis, J.G. Lavin, J. Phys. Chem. B 105 (2001) 10037–10044.
[2] E.C. Weigert, S. Arisetty, S.G. Advani, A.K. Prasad, J.G. Chen, J. New Mat. Electrochem. Systems 11 (2008) 243–251.
[3] N. Liu, K. Kourtakis, J.C. Figueroa, J.G. Chen, J. Catal. 215 (2003) 254–263.
[4] H.H. Hwu, J.G. Chen, J. Phys. Chem. B 107 (2003) 2029–2039.
[5] M.B. Zellner, J.G. Chen, Catal. Today 99 (2005) 299–307.
[6] E.C. Weigert, A.L. Stottlemyer, M.B. Zellner, J.G. Chen, J. Phys. Chem. C 111 (2007) 14617–14620.
[7] H.H. Hwu, J.G. Chen, Surf. Sci. 536 (2003) 75–87.
[8] A. Hamnett, Catal. Today 38 (1997) 445–457.
[9] R. Parsons, T.J. VanderNoot, J. Electroanal. Chem. 257 (1988) 9–45.
[10] A. Hamnett, B.J. Kennedy, Electrochim. Acta 33 (1988) 1613–1618.
[11] M.M.P. Janssen, J. Moolhuysen, Electrochim. Acta 21 (1976) 869–878.
[12] J.G. Chen, M.D. Weisel, Z.M. Liu, J.M. White, J. Am. Chem. Soc. 115 (1993) 8875–8876.
[13] B. Fruhberger, J.G. Chen, J. Am. Chem. Soc. 118 (1996) 11599–11609.
[14] B. Fruhberger, J.G. Chen, Surf. Sci. 342 (1995) 38–46.
[15] N. Liu, S.A. Rykov, J.G. Chen, Surf. Sci. 487 (2001) 107–117.
[16] S.T. Oyama, The Chemistry of Transition Metal Carbides and Nitrides, Blackie Academic and Professional, Glasgow, 1996.
[17] H.H. Hwu, J.G. Chen, Chem. Rev. 105 (2005) 185–212.
[18] R. Levy, M. Boudart, Science 181 (1973) 547–549.
[19] R. Ganesan, D.J. Ham, J.S. Lee, Electrochem. Commun. 9 (2007) 2576–2579.
[20] R. Ganesan, J.S. Lee, Angew. Chem. Int. Ed. 44 (2005) 6557–6560.
[21] S. Izhar, M. Yoshida, M. Nagai, Electrochim. Acta 54 (2009) 1255–1262.
[22] M.K. Jeon, K.R. Lee, W.S. Lee, H. Daimon, A. Nakahara, S.I. Woo, J. Power Sources 185 (2008) 931.
[23] C.A. Angelucci, L.J. Deiner, F.C. Nart, J. Solid State Electrochem. 12 (2008) 1599–1603.
[24] H.J. Zheng, Z.H. Gu, J.H. Zhong, W. Wang, J. Mater. Sci. Technol. 23 (2007) 591–594.
[25] D.J. Ham, Y.K. Kim, S.H. Han, J.S. Lee, Catal. Today 132 (2008) 117–122.
[26] Y. Hara, N. Minami, H. Itagaki, Catal Appl. A: Gen. 323 (2007) 86–93.
[27] G.J. Lu, J.S. Cooper, P.J. McGinn, J. Power Sources 161 (2006) 106–114.
[28] H. Meng, P.K. Shen, Z.D. Wei, S.P. Jiang, Electrochem. Solid State Lett. 9 (2006) A368–A372.
[29] M. Nagai, M. Yoshida, H. Tominaga, Electrochim. Acta 52 (2007) 5430–5436.
[30] X. Jiang, J.E. Parmeter, C.A. Estrada, D.W. Goodman, Surf. Sci. 249 (1991) 44–60.
[31] T.D. Jarvi, E.M. Stuve, Fundamental Aspects of Vacuum and Electrocatalytic Reactions of Methanol and Formic Acid on Pt Surfaces, Wiley-VCH Inc., 1998.
[32] J.G. Chen, C.A. Menning, M.B. Zellner, Surf. Sci. Rep. 63 (2008) 201–254.
[33] J.F. Moulder, Handbook of X-Ray Photoelectron Spectroscopy, Physical Electronics, Minn, Eden Prairie, 1995.
[34] J.X. Wang, S.F. Ji, J. Yang, Q.L. Zhu, S.B. Li, Catal. Commun. 6 (2005) 389–393.
[35] H. Chhina, S. Campbell, O. Kesler, Electrochem. Soc. 154 (2007) B533–B539.
[36] T. Ioroi, N. Fujiwara, Z. Siroma, K. Yasuda, Y. Miyazaki, Electrochem. Commun. 4 (2002) 442–446.